Renewable and Sustainable Energy Reviews 81 (2018) 93–106

Contents lists available at ScienceDirect

Renewable and Sustainable Energy Reviews

journal homepage: www.elsevier.com/locate/rser

Attenuation processes of solar radiation. Application to the quantification of direct and diffuse solar irradiances on horizontal surfaces in Mexico by means of an overall atmospheric transmittance

Antonio J. Gutiérrez-Trashorras[a,*], Eunice Villicaña-Ortiz[b,1], Eduardo Álvarez-Álvarez[a], Juan M. González-Caballín[a], Jorge Xiberta-Bernat[a], María J. Suarez-López[a]

[a] Departamento de Energía, Escuela Técnica Superior de Ingenieros de Minas, Universidad de Oviedo, C/ Independencia, 13, 2a Planta, 33004 Oviedo, Spain
[b] Departamento de Ingeniería de la Energía, Universidad de Ingeniería y Tecnología, Lima, Peru

ARTICLE INFO

Keywords:
Analytical models
Scattering and absorption
Direct and diffuse
Atmospheric and climate parameters
Solar radiation
Renewable energy
Sustainable energy

ABSTRACT

Quantifying incident solar radiation on a surface is a complex task that requires the knowledge of geometric, geographical, astronomical, physical and meteorological characteristics of the location.

The aim of this paper is to analyze the attenuation processes of the solar radiation and to review the scientific works in this field, specifically the analytical models for solar irradiance calculation, as well as to establish an alternative method to compute the magnitude of the overall atmospheric transmittance.

Analytical models have been developed since 1940 and they have been improving in precision and complexity. Up until now, the Bird & Hulstrom model is the most complete and accurate of them all. The main disadvantage of this model is that a great number of equations and parameters such as temperature, sunshine hours, humidity, etc. are required.

In this paper, a very fast and accurate new method is developed to quantify solar irradiances at any site. The analysis shows that the parameters required are only the type of climate, altitude and state of the atmosphere. This method also allows to quantify the influence of the turbidity degree in both direct and diffuse irradiances. That information is essential to select which solar technologies are suitable in each place.

As an application, the new method has been implemented and characterized in Mexico. Solar energy is an abundant resource in Mexico, and there are some studies about the solar energy potential in that country, but the influence of physical and meteorological factors on the solar radiation have not been related. In this study, the meteorological information of 74 weather stations located in different climates of the country were used to determine the parameters required. The results have been validated with experimental data available for different locations.

1. Introduction

The sun emits energy in the form of electromagnetic radiation that travels from the sun's core to the Earth's surface. Along this pathway, solar radiation is modified mainly due to the variation in the distance between the sun and the Earth (eccentricity of the ellipse) and the attenuation processes in the atmosphere, which cause the decrease of radiation along the path [1,2].

Accurately quantifying the incident solar radiation on a surface is a complex task that requires analyzing geometric, geographical, astronomical, physical and meteorological characteristics of the site of study. The phenomena occurring in the Earth's atmosphere are difficult to determine because the concentrations of particles and molecules present in it are highly variable. These concentrations cause the radiation attenuation processes and define the degree of cloudiness – the greater the cloudiness, the more intense the attenuation process. The parameter used to quantify the solar radiation attenuation is known as atmospheric transmittance. Transmittance of a medium is defined as the ratio between the transmitted energy and the incident one upon it. This parameter is really important in the design and implementation of large scale solar energy plants. In practice, this can be

Abbreviations: ANN, Artificial Neural Network; GIS, Geographic Information System; NASA, National Aeronautics and Space Administration; OAT, Overall atmospheric transmittance; RMSE, Root Mean Square Error Measurement units; Å, angstrom; μm, micrometer; masl, meters above sea level; W/m^2, watt per square meter

* Corresponding author.
E-mail address: gutierrezantonio@uniovi.es (A.J. Gutiérrez-Trashorras).
[1] Departamento de Energías Renovables, Universidad Tecnológica del Centro de Veracruz, Mexico.

http://dx.doi.org/10.1016/j.rser.2017.07.042
Received 29 June 2016; Received in revised form 28 June 2017; Accepted 10 July 2017
Available online 20 July 2017
1364-0321/

determined by using particle gauges [3] and/or mathematical models applied to meteorological measurements records.

Du et al. reviewed scientific works on solar energy from 1992 to 2011 using bibliometric techniques based on databases of the Science Citation Index and the Social Science Citation Index [4]. Solar energy markets and policies were discussed in [5] and [6].

As regards the quantification of solar radiation, there are three techniques to calculate its intensity: by means of instrumentation, with satellite images, and using physical and empirical irradiance models; as well as combinations of these.

The use of instrumentation (pyranometers, pyrheliometers, heliographs, etc.) is a reliable technique; though it requires the installation of equipment for recording measurements covering large areas and long periods of time to establish a type year. It is a tedious and very expensive technique [7]. Islam et al. presented actual measurements of direct solar radiation –direct beam radiation– in Abu Dhabi with the meteorological conditions encountered during the measurement throughout the year [8,9] Gherboudj & Ghedira assessed the solar energy potential in the United Arab Emirates using remote sensing and weather forecast data [10].

Determining the solar radiation and the shadows effect more accurately is possible by using and processing the satellite images. However, its use is limited because of its high cost [11]. In [12], the solar energy potential of the western Himalayan Indian state of Himachal Pradesh was evaluated using an algorithm of Waikato Environment for Knowledge Analysis in Artificial Neural Network (ANN) based on a prediction model. In that paper, a correlation was developed between the NASA satellite data and the ground measured global solar radiation data to find values close to the ground measured global solar radiation for different locations. Sorapipatana [13] evaluated the solar energy potential in Thailand using a satellite technique. The results showed that the average solar radiation depends more on geographic features than on the seasonal changes.

The utilization of physical and empirical irradiance models based on measurements and data from some regions is suitable to reliably determine solar radiation. Ertekin et al. studied solar radiation data for Antalya in Turkey. They used twenty six models to test the available data applicability for computing the monthly average daily global radiation on a horizontal surface. The models were compared on the basis of statistical error tests [14]. In [15] a review about the solar energy modeling techniques was made. They considered linear and nonlinear artificial intelligence models for solar energy prediction. El Ouderni et al. overviewed the theoretical models of solar flux estimation [16]. Copper and Sproul presented a comparative study about mathematical models in estimating solar irradiance for Australia [17].

Sözen and Arcaklioglu investigated the effect of the relative humidity on the solar potential by using artificial neural-networks (ANN) [18]. Their results showed that the humidity has a negligible effect on the solar potential prediction. Fadare developed an ANN based on a model for the prediction of solar energy potential in Nigeria [19] and Sözen et al. used an ANN for mapping of the solar potential in Turkey [20–22]. Also, Gutierrez-Corea et al. [23] introduced a new methodology using ANN models and based on observations made in parallel by neighboring sensors and values for different variables using up to 900 inputs. The ANN models predict short-term GSI with error rates less than 20% RMSE. The minimum difference between the average error rates obtained with these ANN models presents a 1.06% RMSE improvement on average compared to previous models and studies.

Pan et al. [24] used the empirical Bristow–Campbell model [25] for estimating the solar radiation. In that study, the Bristow–Campbell model was validated by using daily meteorological observations over the Tibetan Plateau of China.

Grindley et al. [26] developed a simple clear-sky irradiance model with good agreements between the predictions and measurements on a minute-by-minute basis for both the global horizontal and diffuse transmittances and those obtained under apparently clear skies. In [24], the extra-terrestrial radiation and clear sky atmospheric transmittance were calculated on a Geographic Information System (GIS) platform.

Recently, Liu et al. [27] have studied the solar irradiance and its prediction interval are forecasted with the aid of a meteorological model for the prediction of the photovoltaic systems generation. The forecasted irradiance showed a slight positive mean bias error in the intra–day forecasting compared with the observation. Kurtz et al. [28] have measured diffuse, direct, and global irradiance using a sky imager. This technique is used for aerosol characterization, cloud detection, and solar forecasting. Global horizontal irradiance RMSE for a year-long data set is in the 9–11% range for per-image data and 6–9% for hourly-averaged data when compared against a solid-state pyranometer. A machine learning algorithm was employed by [29] to predict the horizontal sky-diffuse irradiance and conduct sensitivity analysis for the meteorological variables, but the model is based only on five years of solar irradiance measurements.

A k-nearest neighbor ensemble model has been developed by [30] to generate Probability Density

Function forecasts for intra-hour Direct Normal Irradiance. The proposed model is developed and validated at multiple locations with different local climates and it has high potential to benefit the integration of concentrated solar power plants.

It should be noted that there are very few models that quantify solar radiation considering the effect of the atmospheric transmittance and their use for a particular region first requires a characterization of the physical and meteorological conditions of the place under study. The treatment of all variables makes it essential to use statistical tools and mathematical methods in order to minimize calculations.

Irradiance physical models may have limited results if the appropriate data and model are not employed. In this study, the Bird & Hulstrom model [31] is used as a base to quantify and characterize the solar resources, since it considers the elements that attenuate solar radiation passing through the atmosphere. Specifically, the non-spectral Bird & Hulstrom model, also known as model "C" of Iqbal [32,33] has been used. This model identifies the set of coefficients responsible for the attenuation due to the presence of particles in the Earth's atmosphere.

In this paper, a new method based on the Bird & Hulstrom model is also used to quantify solar radiation at any site according to the type of climate, altitude and state of the atmosphere. The new method significantly reduces the calculation process of the Bird & Hulstrom model and it is applied to obtain the solar energy irradiances in Mexico.

In Mexico, the solar energy is an abundant resource [34–37] although it is a country with very varying climatic conditions. There are some studies conducted by Mexican academic institutions about the solar energy potential in Mexico [38–41], but the influence of physical and meteorological factors on the solar radiation is not related. Consequently, the analysis about the influence these factors is of special interest and the Bird & Hulstrom model is very suitable.

The aim of this paper is to review the attenuation processes of the solar radiation and the analytical models for solar irradiances calculation, as well as to establish an alternative process that simplifies the Bird & Hulstrom model and computes the magnitude of overall atmospheric transmittance. This method is applied to each area of Mexico, in order to quantify and characterize the solar radiation in the whole country and it allows to identify the regions with the greatest potential for harnessing solar energy. This new methodology can be applied to any region in the world.

2. Attenuation processes of solar radiation

The energy emitted by the sun which reaches the Earth has two major features: it is scattered and intermittent. Radiation passing through the atmosphere undergoes changes which make it heterogeneous and intermittently distributed. Meteorological phenomena on Earth's atmosphere cause their variable availability [42].

The solar radiation disposal depends on geographical, astronomical, geometrical, physical and meteorological factors. The astronomical factors are related to the solar constant, solar declination, hour angle and hours of sunshine. The geographic factors depend on the latitude, longitude and altitude of the site [43]. The geometric factors are a function of the surface height and solar azimuth angle [44]. The physical factors are related to the content of water vapor in the atmosphere, the scattering by air molecules and miscible gases, the presence of aerosols [45] and the effect of ozone [46]. Meteorological factors are related to the temperature, precipitation, humidity, etc. [47]. The latter two groups are more difficult to quantify, as they vary continuously, which make them vital factors in accurately establishing the incident energy on the Earth's surface at specific periods of time.

The solar radiation scattering occurs when an electromagnetic wave collides with a particle and part of the incident energy is distributed in space in the form of photons which continue travelling in all directions [32]. Photons are the elements that scatter while the scattering particles are the air molecules. To determine the scattering magnitude the Rayleigh theory, which calculates the dispersion by air molecules with sizes of about 1 Å, is used [33,48].

The absorption of solar radiation is a process that occurs due to the presence of different components in the atmosphere and varies with the wavelength [49]. The main substances that increase absorption are the gases and particles in the air such as water vapor (H_2O) and ozone (O_3), as well as CO_2, N_2O, CO, O_2, CH_4 and N_2. Of these, only those that belong to the group known as uniformly miscible gases (CO, O_2, CO_2, N_2O) produce significant absorption. Concentrations of CO_2, CH_4 and N_2O in the atmosphere are so low that their absorption effect is minimal and therefore can be ignored. As regards N_2, despite being the most abundant gas in the atmosphere, its absorption of solar radiation is limited to a small band of the electromagnetic spectrum (X-rays and high frequencies). Therefore, its absorption is not relevant in the range of wavelengths between 0.3 and 3 µm, the range in which 96.62% of the energy of solar radiation is concentrated [50,32].

Other elements of significant absorption are aerosols [51,52], either of natural origin (marine, mineral, volcanic, biogenetic and cosmic) or from human activity (dust, soot, volatile organic compounds, combustion fumes, ...) [53].

Aerosols are heterogeneous mixtures of solid or liquid particles suspended in a gaseous medium. The size of these particles can range from 0.005 to 20 µm in effective radius. The influence of these substances is crucial in the attenuation process of solar radiation because:

1) They give rise to the formation of clouds [54] and depending on their type and extent, they define the turbidity degree of the sky (the higher the turbidity, the higher the attenuation) [55,56].
2) They are linked to the Earth's climate, as they interact with sunlight and cause changes in the microphysical properties of clouds and their environment [57].

The presence of aerosols in the atmosphere is variable and its density defines the degree of turbidity [58]. This parameter is not equal at all points of the Earth, so it must be defined for each region under study. There are several methods to do this. Some of the best known are the Angström Turbidity Coefficient and the Linke Factor [28,59,60].

The magnitude of the scattering and absorption effects depends on the relative air mass, the intersection of a solar beam with the atmosphere, as well as the substances concentration in the atmosphere [34].

To evaluate these effects it is necessary to estimate the density of each substance per unit cross section throughout the radiation path [32,34]. Calculating these values is a complex task that requires the application of mathematical and statistical models.

3. Review of analytical models for the calculation of solar radiation

Analytical models for the solar irradiances calculation have been developed from 1940 and have been increasing in precision and complexity. This section presents a revision of the most relevant analytical models trying to gage their advantages and limitations.

3.1. Moon's model

In 1940 the engineer Parry Moon elaborated a pioneering model for the calculation of the direct irradiance of the whole band at sea level in which he proposed standard radiation curves [61]. He subdivided the solar spectrum into six wavelength ranges and evaluated five different solar altitude angles (90°, 30°, 19°, 14° and 11°). As for the characterization of the absorption and dispersion phenomena, Moon identified five different transmittances due to the dispersion of dry air, dust, ozone and dispersion and absorption by water vapor. The direct irradiation was calculated as the product of the five of them. Moon calculated the transmittance of dry air based on measurements made in 1915 by Fowle on Mount Wilson [62] with the solar spectrum wavelength ranging from 0.35 to 0.50 µm. The values obtained revealed that the air transmittance depends exponentially on the inverse of the wavelength fourth power. Likewise, he calculated the transmittance due to the dispersion by water vapor. To determine the transmittance due to the absorption of water vapor, Moon took the data tabulated by Fowle, obtained at an altitude of 1730 masl [62]. As for dust transmittance, Moon formulated another exponential expression considering an average atmosphere of 800 dust particles per cm^3. Finally for the transmittance due to ozone, Moon proposed an equation considering the attenuation coefficient $(k_{o\lambda})$ previously measured by Läuchi [63].

Despite the importance of this model, as the values of dust, ozone and precipitable water level for Washington were assumed, the results obtained were only valid for this area and for the direct irradiance.

3.2. Reddy's model

In 1971 Reddy presented a more complex model to estimate the total daily global irradiation (H) (Eq. (1)). This model introduced a notable improvement, including in its calculation the daily sun hours (n), the average duration of the day during the month (N), the ratio of rainy days (J), the relative humidity (R) and the relationship between length of day and latitude (K) [64,65].

$$H = K\left[\left(1 + 0.8\frac{n}{N}\right)\frac{(1 - 0.2J)}{R}\right] \tag{1}$$

The model of Reddy involved a significant improvement since it introduced the climatology as a variable to estimate the global radiation of a place, but it lacked specific formulations for the calculation of direct and diffuse solar irradiation.

3.3. ASHRAE model

The American Society of Heating, Refrigeration and Air Conditioning Engineers (ASHRAE) published in 1972 a model to determine the solar irradiance in northern hemisphere [66]. This model is the result of the work done by Threlkeld and Jordan in 1958 [67] which is based on the technique developed by Moon for the direct radiation calculation of the entire spectral band.

To carry out the calculation of the different transmittances, they devised a basic clear atmosphere composed of 200 dust particles per cm^3, an ozone concentration of 0.25 cm under normal conditions of pressure and temperature and an average monthly value of the amount of precipitable water obtained from the measurements made by Threlkeld in different parts of the United States. The values of the solar constant *(A)*, the optical coefficient of apparent attenuation *(B)* and the relative mass of the air (m_r) are used to estimate the direct radiation (G_{bn}) (Eq. (2)).

$$G_{bn} = Ae^{(-Bm_r)} \tag{2}$$

The diffuse radiation (G_d) (Eq. (3)) is calculated by means of a coefficient called "number of clarity" (C_n).

$$G_d = G_{bn}C_n \tag{3}$$

The values of these parameters are tabulated for each month of a year and for a clear standard atmosphere [33]. The simplicity of this model is an advantage and it provides both direct and diffuse irradiations. However, it is only applicable to clear atmospheres.

3.4. Lacis & Hansen model

Lacis & Hansen presented a model to estimate the global irradiance in 1973 [68]. According to Eq. (4), this model determines the total irradiance as a function of the solar constant (G_{sc}), the zenith angle (θ), the absorptivity of the ozone (a_o), the absorptivity of the water vapor (a_w), the atmospheric albedo (ρ'_a) and the soil albedo (ρ_g).

$$G = Gsc(\cos\theta)\left[\frac{0.647 - \rho'_a - a_o}{1 - 0.0685\rho_g} + 0.353 - a_w\right] \tag{4}$$

For the calculation of the transmittance due to the absorption of the ozone, Lacis and Hansen evaluate the absorption in two bands of the solar spectrum (the ultraviolet one and the visible one). These calculus are based on the measurements made by Manabe and Strickler [69].

This model is extremely simple and interesting because of the way in which the transmittance value due to ozone is obtained. The results indicate an overestimation of 8% in the global irradiance when the air mass is equal to 1, which is usually an acceptable value. However, it does not present a methodology for determining the direct irradiance.

3.5. Hottel's model

In 1976 Hottel presented a new model to calculate both direct and diffuse irradiance in a "clear atmosphere" [70,71]. The processes of absorption and dispersion that occur in the atmosphere are taken into account for the first time by means of a new coefficient named transmittance (τ_b). The direct radiation also depends on the solar constant (G_{on}) and the zenith angle (θ) (Eq. (5)). This model considers four types of climates and a standard atmosphere (medium latitude and without contamination by pollution).

$$G_{cb} = G_{on}\cdot\tau_b\cdot\cos\theta \tag{5}$$

The transmittance coefficient (τ_b) is obtained by Eq. (6):

$$\tau_b = a_0 + a_1 e^{-\left(\frac{k}{\cos\theta}\right)} \tag{6}$$

where parameters a_0, a_1 and k are defined by the climatic conditions for a standard atmosphere of 23 km of visibility (clean and clear atmosphere).

Diffuse irradiance is obtained by Eq. (7):

$$G_{cd} = G_{on}\cdot\tau_d\cdot\cos\theta \tag{7}$$

where τ_d is the transmittance coefficient for the diffuse component and is given by Eq. (8):

$$\tau_d = 0.2710 - 0.2939\cdot\tau_b \tag{8}$$

This model is interesting for its simplicity, but it only applies to clear atmospheres.

3.6. Davies & Hay model

In 1978 Davies and Hay presented in the First Canadian Solar Radiation Data Workshop a model for the calculation of both direct (G_b) and diffuse irradiance (G_{as}) [72]. The model also considers the fraction of irradiance due to the multiple reflections between the soil and the atmosphere (G_{dm}). The global irradiance (G_{mdh}) is given by the sum of these three solar components (Eq. (9)).

$$G(MDH) = G_b(MDH) + G_{as}(MDH) + G_{dm}(MDH) \tag{9}$$

The direct irradiance (G_b) is calculated as a function of the solar constant, the zenith angle, the transmittance due to the presence of precipitable water vapor, and the transmittances due to the absorption of ozone, the aerosol dispersion and the air molecules.

The transmittance due to the absorption of the ozone depends on the optical depth of the ozone.

For the transmittance due to the presence of aerosols, Davies and Hay introduce a new factor (k_{MDH}) representing the characteristics of an aerosol. The transmittance due to the absorption of water vapor depends on the optical depth of the precipitable water.

The diffuse irradiance (G_{as}) contemplates the analysis of the dispersion of the aerosols by albedo $(\omega_o = 00.98)$, as well as the aerosol forward scattering ratio (F_c), which is the percentage of energy due to the dispersion by aerosols that is directed towards the Earth´s surface $(F_c = 0.85)$. Finally, the fraction of the diffuse irradiance due to the multiple reflections between the sky and the atmosphere is considered (G_{dm}).

This irradiance is calculated from the albedos of the soil and the atmosphere.

This model significantly improves the previous ones and was the first one to treat the direct and diffuse irradiance separately. Its limitations were that it does not present a method for the treatment of the transmittance of aerosols and that it requires tabulated values for the effects produced by air molecules.

3.7. Hoyt's model

Also in 1978, Hoyt published a model for the calculation of the global irradiance (G_{global}) from the sum of direct irradiance (G_b) and diffuse irradiance. The latter is determined by two effects: the aerosol dispersion (G_{dra}) and multiple reflections between soil and atmosphere (G_{dm}) [73] (Eq. (10)).

$$G_{global} = G_b + G_{dra} + G_{dm} \tag{10}$$

Hoyt proposed different expressions to determine each component from the analysis of different radiation sources, such as water vapor, carbon dioxide, ozone, oxygen and aerosols. For the calculation of direct irradiance (G_b), Hoyt proposed an equation including the solar constant (G_{sc}), zenith angle (θ), and dispersion by aerosols (τ_{as}) and by pure air (τ_r) (Eq. (11)).

$$G_b = G_{sc}\cos\theta\left(1 - \sum_{i=1}^{5} a_i\right)\tau_{as}\tau_r \tag{11}$$

where (a_i) is a one-factor term for each of the above mentioned attenuation sources.

The evaluation of the transmittance due to the presence of water vapor (a_1) is based on values obtained by Yamamoto [74]. The transmittance due to the presence of carbon dioxide (a_2) is calculated from the values obtained by Burch [75]. For the transmittance due to the absorption of ozone (a_3), Hoyt establishes an equation based on the works of Manabe and Strickler [70]. The calculation of the transmittance due to the presence of molecules such as oxygen (a_4) is referred to the mass of air corrected by pressure (m_a). Finally, to evaluate the transmittance due to aerosol absorption (a_5), tabulated values of the turbidity coefficient of Angtrom [76,77] are used. To do that, Hoyt introduces a novel analysis which considers the aerosol dispersion behavior depending on the turbidity coefficient of Angtrom. Hoyt proposes Eq. (12) for the transmittance due to the dispersion by air molecules.

$$\tau_r = [f(m_a)]^{m_a} \tag{12}$$

where parameter $f(m_a)$ is tabulated as a function of the mass of air corrected by pressure (m_a)[74].

The diffuse irradiance is calculated by adding two mentioned terms $(G_{dra} + G_{dm})$, aerosol dispersion (G_{dra}) (Eq. (13)) and multiple reflections between soil and atmosphere (G_{dm}) (Eq. (14)). For the latter, the value of the atmospheric albedo (ρ_g) is used.

$$G_{dra}(Hoyt) = G_{sc}\cos\theta\left(1 - \sum_{i=1}^{5} a_i\right)[(1-\tau_r)0.5 + (1-\tau_{as})0.75] \tag{13}$$

$$G_{dm}(Hoyt) = (G_b + G_{dra})\rho_g\left[1 - \sum_{i=1}^{5} a'_i\right]\cdot[(1-\tau'_r)0.5 + (1-\tau'_{as})0.25] \tag{14}$$

This model is one of the most complete, however it has the disadvantage that its application is tedious and some of the values are calculated from tabulated data of reference regions. That is the reason why the application of Hoyt´s model has been restricted to places where no information on atmospheric components is available.

3.8. Atwater & Ball model

In 1978 M.A. Atwater & J.T. Ball presented a rigorous model for the direct irradiance (G_b) and also evaluated the diffuse irradiance [78]. A clear sky equivalent to a visibility of 23 km (extreme clarity) was considered to calculate the direct irradiance (Eq. (15)) which depends on the solar constant (G_{sc}), the zenith angle (θ) and the transmittances due to the molecular effects (τ_b), water vapor (a_w) absorption and aerosols (τ_a).

$$G_b = G_{sc}(\cos\theta)(\tau_b - a_w)\tau_a \tag{15}$$

In order to determine the transmittance of all molecular effects (τ_b), the model is based on the analysis made by McDonald [79] which does not include the transmittance due to the absorption of water vapor. The presence of ozone is not evaluated individually. It is included into the general molecular effects.

The global irradiance is obtained taking into account the soil and atmospheric albedos. The latter is considered equal to 0.0685, which is the value obtained by Lacis and Hansen for a clear atmosphere.

In spite of its rigor and simplicity, this model is limited to atmospheric conditions of extreme clarity, since it does not consider the transmittance due to the presence of aerosols. It is not applicable for skies with turbidity.

3.9. Watt's model

Another of the solar models published in 1978 was Watt's model [80]. This author developed a methodology for the calculation of direct and diffuse irradiance based on Moon's studies.

The direct irradiance (G_b) depends on the solar constant (G_{sc}) and the zenith angle (θ). Watt considered the attenuating effects of the different transmittances: absorption of water vapor (τ_{wa}), absorption and dispersion of dry air (τ_{AS}), absorption of ozone (τ_o), absorption and dispersion of aerosols in the entire radiation spectrum for both low (τ_{aL}) and high layers (τ_{aU}) of the earth's atmosphere. He also considered the dispersion by water vapor (τ_{ws}) (Eq. (16)).

$$G_b = G_{sc}\cos\theta_{wa}\tau_{AS}\tau_o\tau_{ws}\tau_{aL}\tau_{aU} \tag{16}$$

An empirical expression to calculate the transmittance due to water absorption was obtained using the data recorded in the Handbook of Geophysics and Space Enviroments [81] with good results. In this model, Watt included the analysis of the optical depth which he called "path length modifiers", a similar concept to the mass of air, depending on the components (dry air, water vapor, aerosols and ozone) and the altitude.

Finally, for the calculation of the diffuse irradiance, Watt considered all the scattering effects occurring in the atmosphere, the atmospheric and the soil albedos.

This is a rigorous complete model based on meteorological parameters, allowing reliable results. The values of global radiation obtained are overestimated by 7% for air masses equal to 1. The application is complex because it requires data like the turbidity of aerosols in the upper layers of the atmosphere, which are difficult to obtain. However, it represents an important advance in the analysis of radiation.

3.10. Bird & Hulstrom model and improvements

The non-spectral Bird & Hulstrom model (1981) or model “C” of Iqbal [34] is more complete and accurate than the models previously presented and it is explained in more detail. This model determines the total irradiance (I_{TH}), from the amount of direct irradiance (I_{DH}) and diffuse irradiance (I_{dH}) on a horizontal surface for the entire frequency band [82] (Eq. (17)).

$$I_{TH} = I_{DH} + I_{dH} \tag{17}$$

The direct irradiance (I_{DH}) on a horizontal surface is determined from Eq. (18).

$$I_{DH} = 0.9662\cdot C_r\cdot\tau_r\cdot\tau_o\cdot\tau_g\cdot\tau_w\cdot\tau_a\cdot senA \tag{18}$$

being:

C_r: Value of daily solar constant (W/m^2).
τ_r: Transmittance by scattering due to air molecules.
τ_0: Transmittance due to absorption of ozone (O_3).
τ_g: Transmittance due to absorption by the uniform gases mixture (CO_2 and O_2).
τ_w: Transmittance due to absorption of water vapor.
τ_a: Transmittance due to absorption and scattering by the presence of aerosols.

0.9662: Correction factor which adjusts the wavelength range of the solar spectrum (0.3–3 µm).

A: solar altitude angle in degrees.

The position of the sun relative to a point on the Earth's surface has an angle of incidence with reference to the horizontal plane at the same point which is called the solar altitude angle *(A)*.

The value of the daily solar constant varies according to Eq. (19) [34].

$$C_r = C\cdot\left(1 + 0.033\cdot\cos\frac{360\cdot n}{365}\right) \tag{19}$$

where n is the Julian day and C is the normalized solar constant, C =

1367 W/m^2 (average annual solar radiation arriving at the outer limits of the Earth's atmosphere).

The transmittance by scattering (τ_r) evaluates the change of direction experienced by solar radiation due to the presence of air molecules (Eq. (20)).

$$\tau_r = e^{-0.0903 \cdot m_a{}^{0.84}(1+m_a-m_a{}^{1.01})} \tag{20}$$

where m_a is the optical air mass [34], which depends on the total air pressure (P_T), the relative air mass (m_{rel}), the solar altitude angle (A) and the altitude (z).

The transmittance due to the absorption of ozone (τ_O) depends on the relative air mass and the thickness of the ozone layer (Lo) of the atmosphere [34] (Eq. (21)).

$$\tau_o = 1 - \left[0.1611 \cdot [(Lo \cdot m_{rel})(1 + 139.48 \cdot Lo \cdot m_{rel})^{-0.3035}] + \frac{0.002715 \cdot Lo \cdot m_{rel}}{1 + 0.044 \cdot Lo \cdot m_{rel} + 0.003 \cdot (Lo \cdot m_{rel})^2}\right] \tag{21}$$

The transmittance due to absorption by the uniform gases mixture (τ_g) is determined by Eq. (22) [34].

$$\tau_g = e^{-0.0127 \cdot m_a{}^{0.26}} \tag{22}$$

The transmittance due to absorption of water vapor (τ_w) is obtained from Eq. (23) [34].

$$\tau_w = 1 - \frac{2.4959 \cdot (WW \cdot m_{rel})}{(1 + 79.034 \cdot WW \cdot m_{rel})^{0.6828} + 6.385 \cdot WW \cdot m_{rel}} \tag{23}$$

WW being the amount of water capable of precipitating vertically [34].

Finally, it was found that aerosols have a strong impact on the atmospheric turbidity [83]. The influence of radiation is important because it can absorb or scatter the incident photons depending on the size of the aerosol.

Mächler parameterization [84] is used to obtain the transmittance due to the presence of aerosols (τ_a) , according to the Iqbal model (Eq. (24)). This parameterization depends on the average particle size *(α)* and the amount of aerosols. The average particle size is 1.3 µm ± 0.2 [85]. The amount of aerosols is measured by the degree of turbidity of the atmosphere (β). This parameter is also called the Angstrom turbidity coefficient and can vary from 0 (extremely clean atmospheres) to 0.5 (extremely turbid atmospheres).

$$\tau_a = 0.12445\,\alpha - 0.0162 + (1.003 - 0.125\,\alpha)\,e^{-\beta\, m_a(1.089\,\alpha+0.5123)} \tag{24}$$

The product of all attenuation coefficients responsible for direct radiation (τ_r, τ_o, τ_g, τ_w and τ_a) is called atmospheric overall transmittance of direct radiation (τ_{total}).

The total diffuse irradiance on a horizontal surface is made up of to three solar components [34] (Eq. (25)):

- Due to scattering by air molecules (Rayleigh diffusion) (I_{dr}).
- Due to the existence of dust particles (aerosols) (I_{da}).
- Caused by multiple reflections between the ground and the atmosphere (I_{dm}).

$$I_{dH} = I_{dr} + I_{da} + I_{dm} \tag{25}$$

Diffuse irradiance due to the existence of air molecules is obtained from Eq. (26).

$$I_{dr} = 0.79 \cdot C_r \cdot \tau_o \cdot \tau_g \cdot \tau_w \cdot \tau_{aa} \cdot 0.5 \cdot \frac{1 - \tau_r}{1 - m_a + m_a^{1.02}} \cdot senA \tag{26}$$

This model assumes that 50% of solar energy is directed toward the Earth's surface due to scattering by air molecules. The transmittance due to absorption by aerosols (τ_{aa}) (Eq. (27)) requires the scattering albedo (ω_o) whose value is 0.9 [31].

$$\tau_{aa} = 1 - (1 - \omega_o)(1 - m_a + m_a{}^{1.06})(1 - \tau_a) \tag{27}$$

The diffuse radiation due to the presence of aerosols is obtained from Eq. (28).

$$I_{da} = 0.79 \cdot C_r \cdot \tau_o \cdot \tau_g \cdot \tau_w \cdot \tau_{aa} \cdot F_c \cdot \frac{1 - \tau_{as}}{1 - m_a + m_a^{1.02}} \cdot senA \tag{28}$$

being:

Fc: percentage of the energy on the Earth's surface due to scattering by aerosols, estimated from Mac`s parametrization (Eq. (29)).

$$F_c = 0.93 - 0.21 \ln m_a \tag{29}$$

τ_{as}: transmission coefficient due solely to diffusion by aerosols, obtained from Eq. (30).

$$\tau_{as} = \frac{\tau_a}{\tau_{aa}} \tag{30}$$

The calculation of diffuse irradiance by multiple reflections *(I_{dm})* requires the reflection coefficients of each different surface (ρ_g). It also requires an evaluation of the atmospheric albedo, ie, multiple reflections between the ground and the sky (ρ'_a) [29] (Eqs. (31) and (32)).

$$I_{dm} = (I_{DH} \cdot senA + I_{dr} + I_{da}) \cdot \frac{\rho_g \cdot \rho_a'}{1 - \rho_g \cdot \rho_a'} \tag{31}$$

$$\rho_a' = 0.0685 + (1 - F_c)(1 - \tau_{as}) \tag{32}$$

As it can be seen, the application of the Bird & Hulstrom model assesses the influence of climatic and meteorological variables, which are responsible for the attenuation of solar radiation, giving very reliable results.

4. Methodology

In this study, a new method is developed based on the non-spectral Bird & Hulstrom model, which is the most complete and accurate of the analytical models presented in the previous section. The new method interpolates the values obtained by Bird & Hulstrom model by means of very simple equations which allow to quantify the solar irradiances at any site according to the type of climate, altitude and state of the atmosphere. This method significantly reduces the calculation process.

As a study case it is applied to Mexico where, to obtain the specific parameters, data from several weather stations along the country were used.

4.1. Data acquisition and processing: weather stations

74 weather stations located in different parts of the country [86] were used to acquire the meteorological information of the different climates of Mexico.

The daily average records of variables such as temperature, sunshine hours, humidity, evaporation, altitude, barometric pressure and rainfall within a period of 20 years were obtained for each weather station. These data are enough to develop the model proposed. Table 1 shows the mean characteristics of the weather stations [87]. Altitude is expressed in meters above sea level (masl).

These stations provide information about the five types of climates predominant in Mexico (warm-humid, sub-humid warm, dry, very dry and sub-humid mild). Weather stations have been classified and located on the digital map of the National Institute of Statistics and Geography [87] (Fig. 1).

Table 1
Weather stations in Mexico.

No.	Station	State	Latitude	Longitude	Altitude (masl)	Temperature (°C)	Relative humidity (%)
1	Acapulco	Guerrero	16°45′47′′	99°44′56′′	3	28	0.75
2	Aguascalientes	Aguascalientes	21°51′12′′	102°17′29′′	1877	19	0.52
3	Altar	Sonora	30°42′52′′	111°50′05′′	397	22	0.56
4	Arriaga	Chiapas	16°14′28′′	93°53′51′′	49	28	0.72
5	Campeche	Campeche	19°50′	90°30′	5	27	0.72
6	Chetumal	Quintana Roo	18°29′	88°18′	9	27	0.77
7	Chihuahua	Chihuahua	28°42′	106°07′	1482	19	0.5
8	Chilpancingo	Guerrero	17°33′	99°30′	1265	23	0.67
9	Ciudad Guzmán	Jalisco	19°43′50′′	103°27′53′′	1515	20	0.66
10	Ciudad Victoria	Tamaulipas	23°44′52′′	99°10′18′′	336	25	0.71
11	Coatzacoalcos	Veracruz	18°11′22′′	94°30′39′′	16	26	0.78
12	Colima	Colima	19°14′32′′	103°43′13′′	444	26	0.58
13	Colotlán	Jalisco	22°06′26′′	103°16′04′′	1736	19	0.55
14	Comitán	Chiapas	16°14′	92°08′	1607	19	0.71
15	Cozumel	Quintana Roo	20°31′	86°56′	4	26	0.8
16	Cuernavaca	Morelos	18°53′32′′	99°14′	1618	21	0.57
17	Culiacán	Sinaloa	24°38′05′′	107°26′26′′	39	25	0.49
18	Durango	Durango	24°05′41′′	104°35′59′′	1872	18	0.64
19	Empalme	Sonora	27°57º	110°48′	12	25	0.59
20	Felipe Carrillo	Quintana Roo	19°34′	88°03′	10	26	0.76
21	Guadalajara	Jalisco	20°42′36′′	103°23′24′′	1551	20	0.61
22	Guanajuato	Guanajuato	21°00′20′′	101°17′08′′	1999	19	0.63
23	Hermosillo	Sonora	29°04′42′′	110°55′48′′	211	22	0.66
24	Hidalgo	Chihuahua	26°55′	105°40′	1785	18	0.57
25	Huajuapan	Oaxaca	17°48′	97°46′	1680	19	0.62
26	Isla	Colima	18°43′	110°57′	34	25	0.71
27	Jalapa	Veracruz	19°30′43′′	96°54′14′′	1360	19	0.46
28	La Paz	BCS	24°07′	110°9′	19	25	0.6
29	Lagos Moreno	Jalisco	21°20′44′′	101°56°40′	1920	19	0.59
30	Loreto	BCS	26°01′	111°20′	7	24	0.66
31	Manzanillo	Colima	19°04′	104°20′	3	27	0.75
32	Matlapa	San Luís Potosí	21°20′	98°50′	133	24	0.79
33	Mazatlán	Sinaloa	23°14′	106°24′	3	25	0.74
34	Mérida	Yucatán	20°57′	89°39′	11	25	0.7
35	Monclova	Coahuila	26°54′30′′	101°25′	615	20	0.48
36	Monterrey	Nuevo León	25°44′11′′	100°18′17′′	515	23	0.65
37	Morelia	Michoacán	19°42′	101°11′	1913	19	0.58
38	Nacozari	Sonora	30°22′	109°41′	1040	13	0.48
39	Nuevo casas	Chihuahua	30°22′	107°57′	1468	17	0.49
40	Oaxaca	Oaxaca	17°04′	96°42′	1519	21	0.64
41	Obregón	Sonora	27°29′	109°55′	38	25	0.69
42	Orizaba	Veracruz	18°51′	97°06′	1259	18	0.78
43	Pachuca	Hidalgo	20°07′42′′	98°44′51′′	2425	15	0.61
44	Piedras Negras	Coahuila	28°42′	100°31′	250	23	0.52
45	Progreso	Yucatán	21°16′33′′	89°39′14′′	2	26	0.7
46	Puebla	Puebla	19°03′	98°10′	2179	16	0.58
47	Puerto Ángel	Oaxaca	15°39′	96°29′	43	27	0.74
48	Puerto Peñasco	Sonora	31°18′03′′	113°32′55′′	61	22	0.63
49	Querétaro	Querétaro	20°35′	100°24′	1881	19	0.56
50	Río Verde	San Luís Potosí	21°55′17′′	99°59′47′′	984	22	0.65
51	Salina Cruz	Oaxaca	16°10′15′′	95°10′45′′	2	28	0.62
52	Saltillo	Coahuila	25°22′35′′	101°10′	1790	18	0.6
53	San Cristóbal	Chiapas	16°44′	92°38′	2115	15	0.82
54	San Luís	San Luís Potosí	22°12′27′′	101°01′20′′	1883	18	0.59
55	Santa Rosalía	BCS	27°17′	112°15′	82	24	0.57
56	Sombrerete	Zacatecas	23°28′	103°39′	2351	16	0.54
57	Soto la Marina	Tamaulipas	23°46′	98°12′	21	26	0.65
58	Tacubaya	México DF	19°24′13′′	99°11′46′′	2309	18	0.57
59	Tampico	Tamaulipas	22°12′	97°51′22′′	25	25	0.78
60	Tamuin	San Luís Potosí	22°01′	98°47′01′′	23	26	0.69
61	Tapachula	Chiapas	14°55′15'	92°15′	118	27	0.74
62	Temosachic	Chihuahua	28°57′	107°49′	1932	12	0.65
63	Tepehuanes	Durango	25°20′16′′	105°43′23′′	1810	16	0.56
64	Tepic	Nayarit	21°29′21′′	104°53′35′′	915	22	0.71
65	Tlaxcala	Tlaxcala	19°18′43"	98°14′39′′	2248	16	0.72
66	Toluca	México DF	19°17′	99°39′	2663	12	0.65
67	Torreón	Coahuila	25°31′11′′	103°25′52′′	1123	22	0.5
68	Tuxpan	Veracruz	20°57′35′′	97°25′08′′	10	25	0.82
69	Tuxtla	Chiapas	16°45′	93°08′	570	26	0.64
70	Valladolid	Yucatán	20°41′24′′	88°12′15′′	27	27	0.74
71	Veracruz	Veracruz	19°09′40′′	96°08′13′′	20	25	0.78
72	Villahermosa	Tabasco	17°59′	92°56′	7	25	0.75
73	Zacatecas	Zacatecas	22°46′42′′	102°33′59′′	2612	16	0.54
74	Zamora	Michoacán	19°59′	102°19′	1562	16	0.59

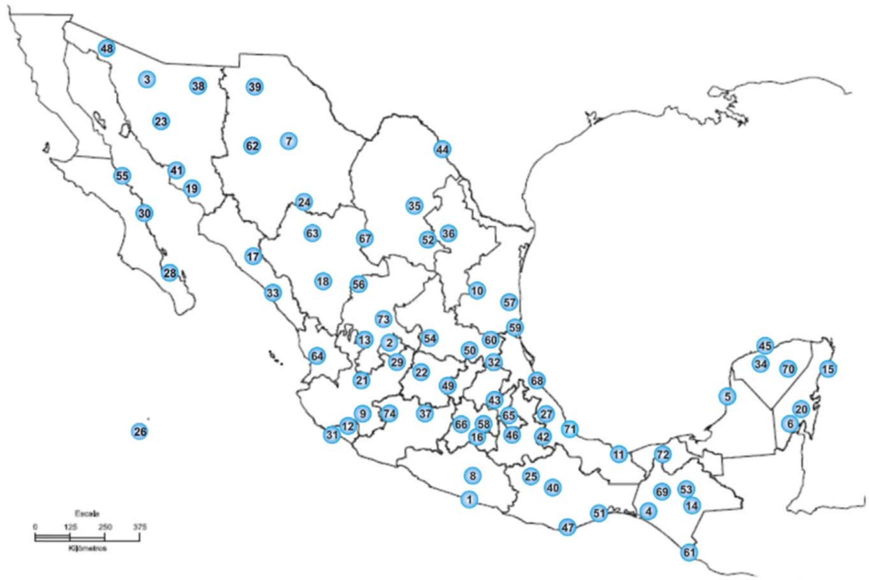

Fig. 1. Location of weather stations.

Table 2
Relationship between type of atmosphere and the turbidity degree.

β	Type of atmosphere
0.0	Extremely clean
0.1	Clear
0.2	Slightly turbid
0.3	Turbid
0.4	Very turbid

4.2. New proposed method: simplification of the Bird & Hulstrom model

Obtaining solar data using the Bird & Hulstrom model is a complex process requiring information about the hypsography, climate and meteorology which is often unavailable. In this paper, a user-friendly method with high accuracy is developed. The Bird & Hulstom model is used as a base, incorporating the adjustments made by Mächler, Leckner, Mac and Iqbal explained in the previous section. Thus, the total solar irradiance (I_{TH}) is the sum of direct (I_{DH}) and diffuse irradiance (I_{dH}) on a horizontal surface (Eq. (17)).

4.2.1. Direct solar irradiance on a horizontal surface (I_{DH})

The direct irradiance (I_{DH}) is obtained by multiplying the amount of energy from the sun by its position relative to a point on the Earth's surface. Eq. (33) is obtained considering that the incident solar energy on the upper layers of the atmosphere is $C = 1367\ \text{W/m}^2$ (solar constant) and the sun's position is determined by means of the solar altitude angle (A).

$$I_{DH} = C \cdot senA \tag{33}$$

I_{DH} obtained from the above equation is imprecise, since it does not take into account that wavelength ranges from 0.3 to 3 μm nor the mitigating effect of radiation passing through a medium. This effect depends on the optical air mass and the processes of absorption and scattering.

The optical air mass is determined from the relative air mass (m_{rel}), while absorption and scattering processes are quantified from the calculation of the different transmittances. For this reason, it is necessary to define a new coefficient of atmospheric transmittance (τ_{OAT}) so that all of these variables can be used establish a global attenuation coefficient, as stated by Moon [61]. Taking into account those considerations, Eq. (33) can be rewritten as Eq. (34), which gives much more accurate values for I_{DH}.

$$I_{DH} = 0.9662 \cdot C \cdot \tau_{OAT} \cdot senA \tag{34}$$

being:

C:	The solar constant.
A:	Solar altitude angle in degrees.
0.9662:	Correction factor which adjusts the wavelength range of the solar spectrum (0.3–3 μm).
τ_{OAT}:	Overall atmospheric transmittance.

Eq. (34) significantly reduces the calculation process of the Bird & Hulstrom model, however, it requires the overall atmospheric transmittance for Mexico. To do so, it is necessary to know the turbidity degree of the atmosphere (β) observed in recent years for the city of Mexico. According to Jáuregui [88], it ranges between 0.2 and 0.4, but when the polar air mass crosses it in dry seasons, the winds associated wash away some of the pollutants and solar radiation reaches the Earth's surface without suffering significant attenuation. For this reason, values of β between 0.0 and 0.4 have been taken [89]. Table 2 shows the relationship between the type of atmosphere and the turbidity degree.

4.2.2. Diffuse solar irradiance on a horizontal surface (I_{dH})

The diffuse solar irradiance (I_{dH}) calculation is more complex than direct solar irradiance, since it requires knowledge of the multiple reflections between the Earth and the atmosphere. This calculation needs to resort to the meteorological observations. In this model, the diffuse irradiance on a horizontal surface depends on the clear sky index (k_d) as this has been proved to give satisfactory results [90]. Therefore, this irradiance is given by Eq. (35).

$$I_{dH} = C \cdot k_d \cdot senA \tag{35}$$

The clear sky index is defined by a diffuse atmospheric coefficient, which is given by the transmittances that affect only diffuse radiation. In these terms, there are several studies which define clarity of the sky corresponding to the diffuse sky fraction as a linear function of an overall atmospheric transmittance [91–94]. The correlations made by these authors and their results provide evidence that this methodology is perfectly acceptable. Consequently, the clear sky index (k_d) can be expressed by Eq. (36), where B and B' are parameters that must be determined by a statistical analysis of a place weather conditions [95].

$$k_d = B - B' \cdot \tau_{OAT} \quad (36)$$

Parameter B is the maximum value of the clear sky index (minimum reflections between the soil and the atmosphere) and B' quantifies how this index varies due to attenuation processes of solar radiation in the atmosphere. In order to obtain the clear sky index, it is necessary to determine the overall atmospheric transmittance.

4.2.3. Overall atmospheric transmittance (τ_{OAT})

To determine the overall attenuation coefficient, Beer's Law is taken into account [96]. This law, applied to solar radiation, establishes that the coefficient of atmospheric transmissibility for direct radiation decreases with the content of particles contained in the atmosphere and the path length of solar radiation [97]. Therefore this coefficient can be expressed by Eq. (37).

$$\tau_{OAT} = a \cdot e^{-(b \cdot m_{rel})} \quad (37)$$

where a and b are parameters for the place of study which define the degree of attenuation experienced by solar radiation in that place and m_{rel} is the relative air mass.

Parameter a represents the flux density of solar radiation (W/m^2) when solar beams enter the atmosphere (maximum value).

Parameter b also called the "attenuation coefficient", is the probability of a solar ray being intercepted at a point within the atmosphere [98].

The relative air mass (m_{rel}) is a purely geometrical relation that evaluates the intersection of a solar beam with the atmosphere, considering the curvature of the Earth.

For solar altitude angles ranging between 30° and 90° the equation to obtain m_{rel} [34] can be simplified as shown in Eq. (38).

$$m_{rel} = \frac{1}{senA + 0.15[93.885 - (90 - A)]^{-1.253}} \approx \frac{1}{senA} \quad (38)$$

Consequently, Eq. (39) is obtained.

$$\tau_{OAT} = a \cdot e^{-\left(\frac{b}{senA}\right)} \quad (39)$$

4.2.4. Obtaining the new model parameters

Obtaining τ_{OAT} from Eq. (39) requires the calculation of parameters a and b. To do so, a correlation analysis by the least squares method between the product of the atmospheric transmittances ($\tau_r \cdot \tau_o \cdot \tau_g \cdot \tau_w \cdot \tau_a$) and the position of the sun (solar altitude angle) at each weather station is done. This involves the calculation of the relative air mass (m_{rel}). The product of those transmittances obtained by the Bird & Hulstrom method is denoted τ_{total}.

In making this correlation, exponential curves confirming Beer's Law are obtained for each weather station and type of atmosphere. τ_{total} decreases exponentially with the length traveled by the solar beams, that is, the lower the solar altitude angle, the greater the solar attenuation (Fig. 2).

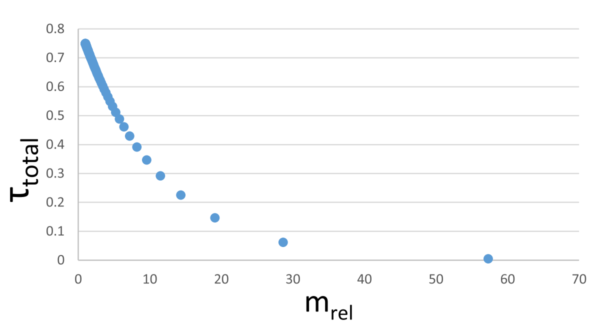

Fig. 2. Correlation curve between the total transmittance and the relative air mass.

By means of these correlations and considering $\tau_{total} = \tau_{OAT}$, parameters a and b can be obtained by least square fitting.

According to the Bird & Hulstrom method and rearranging the Equations from 9 to 16, a new transmittance can be defined (diffuse global transmittance: τ_{diff}), obtaining Eq. (40), equivalent to Eq. (35).

$$I_{dH} = C \cdot \tau_{diff} \cdot senA \quad (40)$$

To calculate the values of parameters B and B' it is necessary to determine the diffuse global transmittance, which is given by the transmittances that affect only the diffuse radiation.

Correlation analyses between the diffuse global transmittance (τ_{diff}) and the overall atmospheric transmittance (τ_{OAT}) for each weather station and type of atmosphere result in a set of straight lines with negative slope. The correlation obtained between the two parameters is linear and very similar to the correlations proposed by Spencer [96].

Considering that the clear sky index (k_d) equals diffuse global transmittance (τ_{diff}), parameters B and B' can be obtained by least square fitting (Eq. (41)).

$$\tau_{diff} = B - B' \cdot \tau_{OAT} \quad (41)$$

5. Results and analysis

Monthly average data from the Mexican weather stations were used to obtain atmospheric transmittances (τ_r, τ_o, τ_g and τ_w) using the Bird & Hulstrom model. Transmittance due to aerosols (τ_a) depends on the different types of atmospheric turbidity quantified by the turbidity degree (β). This procedure was performed for all the weather stations and types of atmosphere to obtain a monthly average of τ_{total}. Similarly, the values relative to astronomical, geometrical and geographical factors, including the corresponding solar altitude and the relative air mass, were taken into account for each weather station and type of atmosphere, as they are necessary for the development of the proposed correlation system.

5.1. Direct solar irradiance parameters

Mean Solar altitude angles in Mexico are greater than 35.6°, therefore the data meet the restriction set for Eq. (38). The different exponential correlations τ_{OAT} versus m_{rel} were obtained for each weather station and type of atmosphere, as well as the respective values of both parameters a and b. The coefficients of determination (R^2) obtained to evaluate the goodness-of-fit were greater than 0.99, indicating that the results are fully satisfactory.

Grouping the weather stations according to the type of climate in Mexico (warm-humid, sub-humid warm, dry, very dry and sub-humid mild), the average values of parameters a and b for each climate and the type of atmosphere were obtained, as well as the overall atmospheric

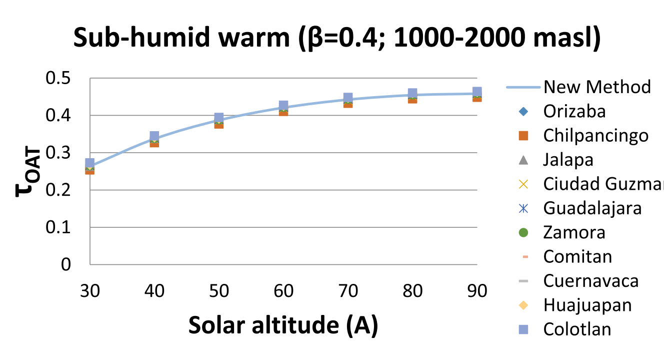

Fig. 3. Overall atmospheric transmittance (τ_{OAT}) versus solar altitude (A) for the sub-humid warm climate, very turbid atmosphere (β = 0.4) and altitude interval 1000–2000 masl.

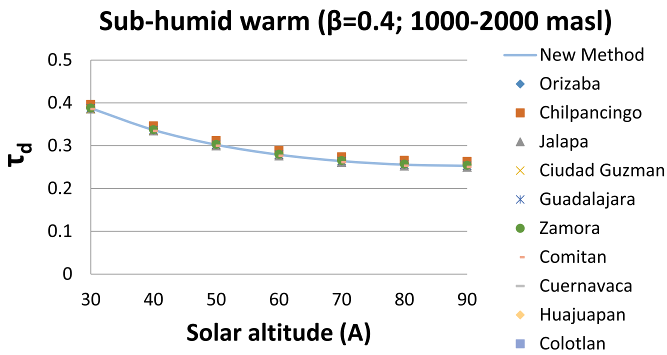

Fig. 4. Diffuse global transmittance (τ_{diff}) versus solar altitude (A) for the sub-humid warm climate, very turbid atmosphere (β = 0.4) and altitude interval 1000–2000 masl.

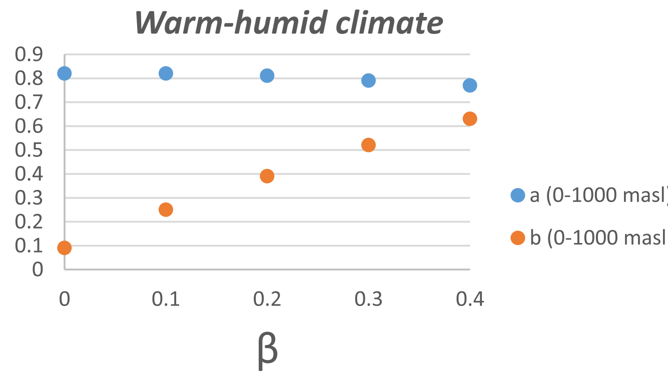

Fig. 5. Parameters a and b versus degree of turbidity of the atmosphere (β) for Warm-humid climate and altitudes lower than 1000 masl in Mexico.

transmittances (τ_{OAT}). The coefficients of determination (R^2) obtained for some climates were less than 0.85, indicating that the results are not very good. Using those values, direct solar irradiances (I_{DH}) were obtained and compared to the values obtained by the Bird & Hulstrom model. Discrepancies were up to 12%, therefore it can be concluded that climate factor alone is not determinant.

As the weather stations are located in different areas of Mexico, some at the sea level and others in high mountain areas, it was concluded that altitudes might be also influence the computation. The path gone through more air mass (atmosphere) is lower than in those stations located in higher altitudes, so that solar radiation is attenuated to a lesser extent than in stations located at sea level. Thus, the country hypsography from the information displayed by the Institute of Geography of the UNAM [98] was assessed. Weather stations were re-classified by climate and altitude intervals (0–1000 masl, 1000–2000 masl and greater than 2000 masl) and new values of the parameters a and b were obtained. The values of these parameters, their dispersion in the territory and their relationship to the climate are described below. Figs. 3 and 4 show the values of the overall atmospheric transmittance (τ_{OAT}) and diffuse global transmittance (τ_{diff}) versus solar altitude (A) for the group of stations corresponding to the sub-humid warm climate, altitude interval 1000–2000 masl and very turbid atmosphere (β = 0.4), as an example. In those figures is also represented the curve obtained by least square fitting (New method).

Similar results were obtained for the other groups of stations. The statistical values obtained indicate that this new classification is correct. In all cases the coefficients of determination (R^2) obtained for each climate, altitude interval and turbidity degree were greater than 0.99.

Table 3 shows the values and confident intervals of parameters a and b by climate, altitude and type of atmosphere with a confidence level of 0.95.

5.1.1. Warm-humid climate

Warm-humid climate is found in greater proportion in the coastal plain of the Gulf of Mexico, the Isthmus of Tehuantepec and the Sierra de los Tuxtlas. The altitude of these areas does not exceed 1000 masl. The values of parameters a and b obtained for the weather stations located in these areas are shown in Fig. 5.

Parameter a is nearly constant (0.8) with the type of atmosphere, slightly decreasing when the turbidity increases; but parameter b ranges approximately from 0.1 to 0.6, increasing almost linearly with the degree of turbidity. Those results are coherent with the definition of a and b parameters. Parameter a is nearly constant, meaning that the energy per unit area when solar beams enter the atmosphere is similar for the different types of atmosphere, and parameter b shows that the probability of a solar ray being intercepted at a point increases when the turbidity degree increases.

5.1.2. Sub-humid warm climate

Sub-humid warm climate has two classifications depending on the altitude, because this climate can be found in various parts of the country, from the north and center of the Coastal Plain of the Gulf of Mexico to the Isthmus of Tehuantepec, Plateau of Zohlaguna and the entire Yucatan Peninsula. In these places, altitudes are up to 1000 masl. This climate also corresponds to the Pacific zone, including the Central Depression of Chiapas, the Pacific Coastal Plain, the Sierra Madre del Sur and Sierra Pacific, where the altitude ranges between 1000 and 2000 masl.

Fig. 6 shows the values of a and b parameters for Sub-humid warm

Table 3
Values and confident intervals of parameters a and b by climate, altitude and type of atmosphere in Mexico.

Climate	β	0	0.1	0.2	0.3	0.4
Warm-humid	a (0–1000 masl)	0.822 ± 0.0058	0.821 ± 0.0056	0.809 ± 0.0056	0.790 ± 0.0055	0.771 ± 0.0053
	b (0–1000 masl)	0.092 ± 0.0012	0.250 ± 0.0022	0.394 ± 0.0037	0.509 ± 0.0045	0.631 ± 0.0058
Sub-humid warm	a (0–1000 masl)	0.821 ± 0.0057	0.820 ± 0.0056	0.811 ± 0.0055	0.790 ± 0.0055	0.763 ± 0.0053
	b (0–1000 masl)	0.090 ± 0.0008	0.239 ± 0.0020	0.391 ± 0.0030	0.512 ± 0.0029	0.620 ± 0.0024
	a (1000–2000 masl)	0.849 ± 0.0059	0.843 ± 0.0058	0.841 ± 0.0058	0.823 ± 0.0057	0.800 ± 0.0056
	b (1000–2000 masl)	0.081 ± 0.0007	0.220 ± 0.0019	0.339 ± 0.0030	0.449 ± 0.0040	0.562 ± 0.0051
Dry	a (0–1000 masl)	0.813 ± 0.0065	0.812 ± 0.0063	0.790 ± 0.0063	0.782 ± 0.0062	0.749 ± 0.0050
	b (0–1000 masl)	0.072 ± 0.0007	0.224 ± 0.0019	0.348 ± 0.0028	0.470 ± 0.0039	0.582 ± 0.0049
	a (1000–2000 masl)	0.831 ± 0.0074	0.820 ± 0.0071	0.819 ± 0.0070	0.800 ± 0.0070	0.783 ± 0.0069
	b (1000–2000 masl)	0.076 ± 0.0007	0.206 ± 0.0020	0.323 ± 0.0032	0.429 ± 0.0043	0.530 ± 0.0053
Very dry	a (0–1000 masl)	0.815 ± 0.0081	0.806 ± 0.0080	0.801 ± 0.0080	0.779 ± 0.0078	0.752 ± 0.0075
	b (0–1000 masl)	0.082 ± 0.0018	0.237 ± 0.0031	0.376 ± 0.0030	0.503 ± 0.0035	0.606 ± 0.0043
Sub-humid mild	a (1000–2000 masl)	0.833 ± 0.0078	0.830 ± 0.0077	0.819 ± 0.0067	0.811 ± 0.0063	0.789 ± 0.0065
	b (1000–2000 masl)	0.071 ± 0.0015	0.214 ± 0.0023	0.333 ± 0.0021	0.445 ± 0.0022	0.542 ± 0.0027
	a (> 2000 masl)	0.843 ± 0.0077	0.842 ± 0.0078	0.840 ± 0.0062	0.827 ± 0.0060	0.811 ± 0.0081
	b (> 2000 masl)	0.073 ± 0.0017	0.203 ± 0.0021	0.314 ± 0.0025	0.417 ± 0.0032	0.516 ± 0.0043

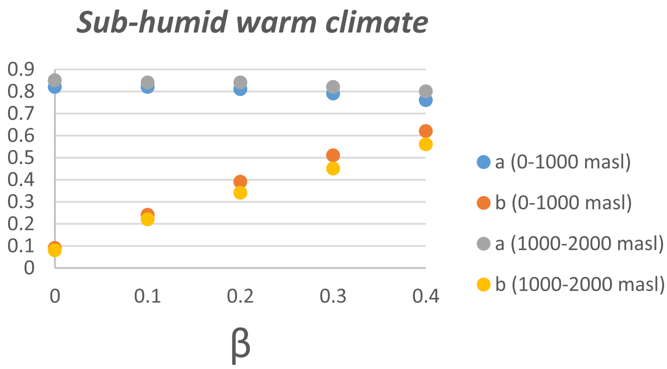

Fig. 6. Parameters a and b versus degree of turbidity of the atmosphere (β) for Sub-humid warm climate and different altitudes in Mexico.

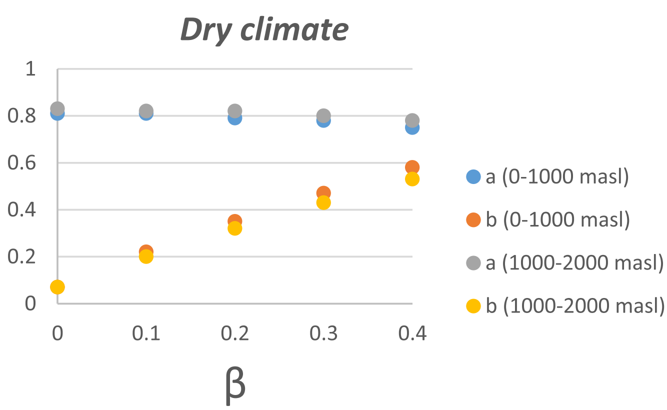

Fig. 7. Parameters a and b versus degree of turbidity of the atmosphere (β) for Dry climate and different altitudes in Mexico.

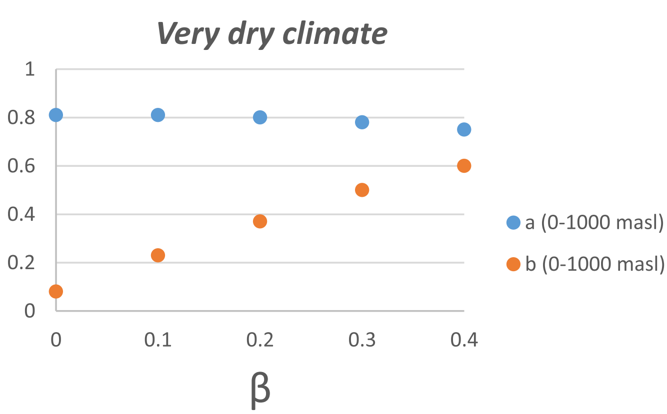

Fig. 8. Parameters a and b versus degree of turbidity of the atmosphere (β) for Very dry climate and altitudes lower than 1000 masl in Mexico.

climate taking into account the different altitudes. The trends are the same as those obtained for warm-humid climate and the higher the altitude (lower distance traveled by solar beams), the higher the a parameter (greater maximum flux density of solar radiation) but the lower the b parameter values (lower attenuation).

5.1.3. Dry climate

The dry climate, although in a small proportion, is present in the coastal area of Yucatan, the Blas basin and part of the Sierra Pacific. In these places the altitude does not exceed 1000 masl. This climate is also present on the Mexican Plateau, Northern Plateau, part of the Sierra Madre Oriental, the Sierra de Guanajuato, the Sierra de Zacatecas and part of the mountainous areas of Baja California, where the altitudes reach 2000 masl.

Fig. 7 shows the values of parameters a and b, taking into account

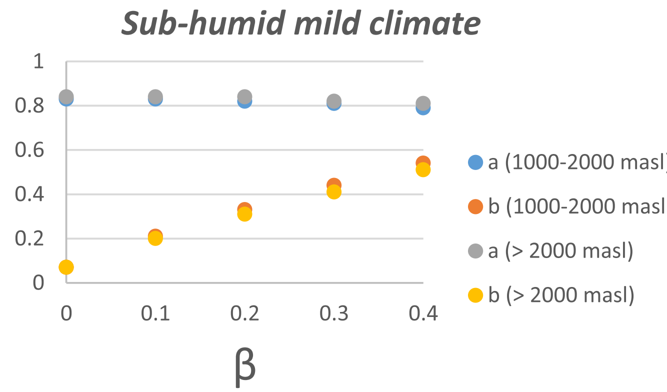

Fig. 9. Parameters a and b versus degree of turbidity of the atmosphere (β) for Sub-humid mild climate and different altitudes in Mexico.

the different altitudes.

5.1.4. Very dry climate

Climate Very dry is mainly located on the Peninsula of Baja California, the Pacific Coastal Plain and the Altar Desert, where altitudes are not higher than 1000 masl. Parameters a and b are shown in Fig. 8.

5.1.5. Sub-humid mild climate

Finally, the Sub-humid mild climate, is located towards the interior of the Country, in the foothills of the Sierra Madre Occidental and Oriental, the Sierra de Durango, the Sierra Madre del Sur, the Sierra de Miahuatlan and the region of the Mixteca, so registered altitudes range from 1000 masl to 2000 masl. This climate is also present in the higher regions of the Sierra Madre Occidental and the Sierra Madre del Sur, as well as the whole Transversal Volcanic System. In these areas the altitude exceeds 2000 masl. Fig. 9 shows the values of parameters a and b for this climate.

5.2. Diffuse solar irradiance parameters

Similarly, the values of parameters B y B' for each type of climate and atmosphere were calculated. Results indicate that the values of these parameters are virtually identical for warm-humid and sub-humid warm climates, as well for dry and very dry climates, with differences lower than 2%. In addition, differences smaller than 1% in B and B' values were obtained for Clear, Slightly turbid, Turbid and Very turbid atmospheres. For this reason, the values of B and B' have been regrouped as shown in Table 4. This table also shows the confident intervals with a confidence level of 0.95.

5.3. Application and validation of the new method

As an example, the application of the new method is firstly used to determine the maximum direct solar irradiance that affects the weather station at Tapachula-Chiapas in February. The average maximum solar altitude (A) is 61° and it is located in an area with predominantly sub-humid warm climate at 118 masl.

With these data and using the corresponding values of a and b from Fig. 6, as well as Eqs. (39) and (34), τ_{OAT} and I_{DH} were obtained respectively.

In Table 5 results are compared with those obtained using the Bird & Hulstrom method for the weather station located in Tapachula-Chiapas.

Table 5 shows that the obtained values of direct solar irradiance are very similar for both the Bird & Hulstrom and the new method with error percentages lower than 2.5%.

The same comparison was done for all the weather stations finding

Table 4
Values and confident intervals of parameters B and B' by climate, altitude and type of atmosphere in Mexico.

Climate		0–1000 masl		1000–2000 masl		> 2000 masl	
	β	0	0.1–0.4	0	0.1–0.4	0	0.1–0.4
Warm-humid &	B	0.261 ± 0.0011	0.570 ± 0.0061	0.272 ± 0.0032	0.571 ± 0.0056		
Sub-humid warm	B′	0.283 ± 0.0033	0.689 ± 0.0071	0.281 ± 0.0019	0.668 ± 0.0081		
Dry &	B	0.312 ± 0.0081	0.569 ± 0.0077	0.303 ± 0.0063	0.567 ± 0.0083		
Very dry	B′	0.343 ± 0.0086	0.691 ± 0.0081	0.322 ± 0.0052	0.681 ± 0.0080		
Sub-humid mild	B			0.299 ± 0.0061	0.572 ± 0.0079	0.283 ± 0.0057	0.583 ± 0.0072
	B′			0.319 ± 0.0070	0.673 ± 0.0064	0.303 ± 0.0062	0.681 ± 0.0081

Table 5
Values of τ_{OAT} and I_{DH} for Tapachula-Chiapas.

β	0	0.1	0.2	0.3	0.4
τ_{OAT}	0.74	0.62	0.52	0.44	0.37
I_{DH} (W/m^2) using the new method	855	712	599	504	433
I_{DH} (W/m^2) using Bird & Hulstrom method	868	724	609	515	440
Error (%)	1.5	1.8	1.6	2.2	1.6

Table 6
Values of k_d and I_{dH} for Tapachula-Chiapas.

β	0	0.1	0.2	0.3	0.4
τ_{diff}	0.05	0.14	0.21	0.27	0.31
I_{dH} (W/m^2) using the new method	63	173	254	322	372
I_{dH} (W/m^2) using Bird & Hulstrom method	66	171	255	322	376
Error (%)	4.3	1.3	0.5	0.0	1.0

Table 7
Values of I_{TH} for Tapachula-Chiapas.

β	0	0.1	0.2	0.3	0.4
I_{TH} (W/m^2) using the new method	918	885	853	825	805
I_{TH} (W/m^2) using Bird & Hulstrom method	934	895	864	837	816
Error (%)	1.7	1.1	1.3	1.4	1.3

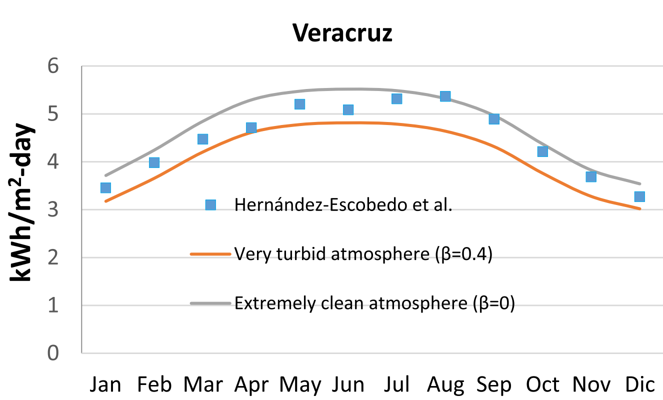

Fig. 10. Comparison between the monthly average solar resource obtained by Escobedo et al. and the new method (extremely clean and very turbid atmosphere) at Veracruz State.

similar error percentages. Therefore, the new method is proved to be a fast and accurate tool to obtain direct solar irradiance.

The advantage of the proposed alternative method is that direct solar irradiance can be calculated quite easily for five types of atmospheres, giving more information about available solar resources. Table 5 shows that the I_{HD} that affects Tapachula Chiapas in February may vary depending on the turbidity of the sky, so that it takes a value of 0.74 for

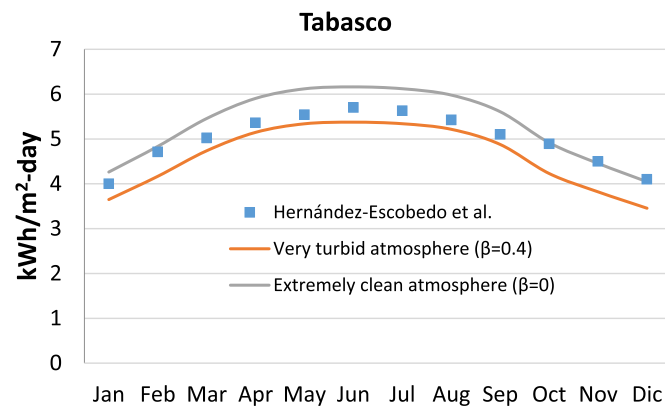

Fig. 11. Comparison between the monthly average solar resource obtained by Escobedo et al. and the new method (extremely clean and very turbid atmosphere) at Tabasco State.

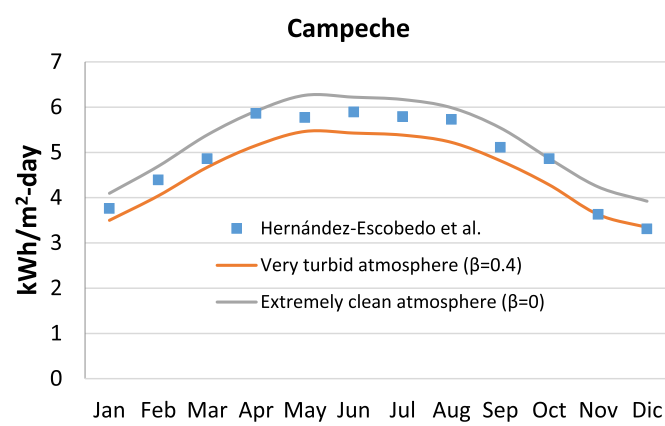

Fig. 12. Comparison between the monthly average solar resource obtained by Escobedo et al. and the new method (extremely clean and very turbid atmosphere) at Campeche State.

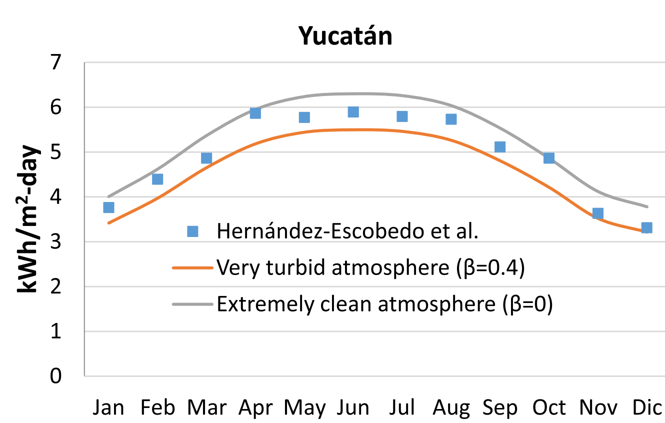

Fig. 13. Comparison between the monthly average solar resource obtained by Escobedo et al. and the new method (extremely clean and very turbid atmosphere) at Yucatán State.

a clean sky, and 0.37 for a very turbid sky. It means that the I_{HD} on a cloudy day can be reduced by up to 50%.

Diffuse solar irradiance has been calculated from Eqs. (40) and (41) taking into account the corresponding values of parameters B and B' from Table 4. The results obtained are compared with the Bird & Hulstrom method, and the values are shown in Table 6.

Table 6 shows that the I_{dD} in Tapachula Chiapas in February varies according to the type of atmosphere, so that on a cloudy day the diffuse solar irradiance can increase up to 5 times with respect to a clear sky.

I_{dD} values obtained with the new method show a maximum variation from the Bird & Hulstrom method of 4.3%. This difference is acceptable to quantify the effects of solar radiation.

The total solar irradiance for this particular case is shown in Table 7. Differences with the Bird & Hulstrom method are lower than 2%.

The same procedure was performed for the different climates and altitudes to obtain the direct, diffuse and total solar irradiance. The results were compared with those obtained with the Bird & Hulstrom model, finding differences between the two models lower than 5%. These results indicate that the new method to compute the availability of solar radiation in Mexico is accurate and very efficient, and that its application does not involve significant errors in the quantification of the solar resource.

The average solar resource (kW h/m^2-day) was also calculated from the solar irradiances obtained with the new method for each type of atmosphere. These results were compared with the monthly average solar energy for some Mexican states, obtained by Hernández–Escobedo et al. [35] from experimental data.

Figs. 10–13 show the monthly average solar resource obtained experimentally and by the new method at Veracruz, Tabasco, Campeche and Yucatán States. As it can be seen, the experimental values fit quite well between the range defined by the turbidity degree (extremely clean and very turbid).

6. Conclusions

This paper analyzes the attenuation processes of the solar radiation taking into account the effects of meteorological and climate conditions. The state of the art in this field is presented, together with a review of the most significant analytical models for solar irradiance calculation. Specifically the Bird and Hulstrom model (the most complete and accurate) is explained in detail, including an overview of its different variations.

Following this revision, a new method based on the atmospheric transmittance is developed. It presents a clear advantage over the traditional Bird & Hulstrom model because it reduces the calculation process to obtain the solar irradiances. Only five simple equations are required depending on the type of climate, altitude and solar altitude instead of the more than fifteen complex equations depending on over ten variables of the Bird & Hulstrom model. This method also allows to quantify the influence of the turbidity degree in both direct and diffuse irradiances. That information is essential to select which solar technologies are suitable in each location.

As an application, the new method has been implemented and characterized in Mexico. Meteorological records of 20 years corresponding to 74 weather stations in Mexico have been used to determine the parameters required. The results obtained for the overall atmospheric transmittance showed that the type of climate is not the only variable that determines the attenuation; the geography of the site was found to be another important element for the quantification. Thus, to determine the definitive parameters employed by the new method, the five types of climates predominant in Mexico have been considered, together with three altitude ranges.

The results show variations smaller than 5% when compared to the Bird & Hulstrom model and they have been also validated with experimental data available for different locations. The characteristics of the new method make it a fast, simple and reliable procedure to estimate the solar irradiance, especially for those places where direct information is not available.

The numerical values of the parameters have been obtained specifically for Mexico, but it should be applicable elsewhere. Nonetheless, the grouping in climates and altitudes should be further tested, being the most sensitive aspect of the methodology.

References

[1] Prieto JI Capitulo II. Disponibilidad de la Energía Solar. Universidad de Oviedo, Departamento de Máquinas y Motores Térmicos. Mayo. Oviedo, España; 2008.
[2] Martínez AI de Licenciatura Tesis. Sistemas fotovoltaicos conectados a red. Planta Fotovoltaica 20 MW Portusa. Departamento de Energía. Universidad de Oviedo. Oviedo, España; 2007.
[3] Medidor de partículas KM3887. Manual de equipos de medida para la industria, el comercio y la investigación. Albacete. España; 2011.
[4] Du H, Li N, Brown MA, Peng Y, Shuai Y. A bibliographic analysis of recent solar energy literatures: the expansion and evolution of a research field. Renew Energy 2014;66:696–706.
[5] Timilsina Govinda R, Kurdgelashvili Lado, Narbel Patrick A. Solar energy: markets, economics and policies. Renew Sustain Energy Rev 2012;16.1:449–65.
[6] Solangi KH, Islam MR, Saidur R, Rahim NA, Fayaz H. A review on global solar energy policy. Renew Sustain Energy Rev 2011;15(4):2149–63.
[7] Fariba B, Ali A, Ahmad R. Empirical models for estimating global solar radiation: a review and case study. Renew Sustain Energy Rev 2013;21:798–821.
[8] Islam MD, Kubo I, Ohadi M, Alili AA. Measurement of solar energy radiation in Abu Dhabi, UAE. Appl Energy 2009;86(4):511–5.
[9] Islam MD, Alili AA, Kubo I, Ohadi M. Measurement of solar-energy (direct beam radiation) in Abu Dhabi, UAE. Renew Energy 2010;35(2):515–9.
[10] Gherboudj I, Ghedira H. Assessment of solar energy potential over the United Arab Emirates using remote sensing and weather forecast data. Renew Sustain Energy Rev 2015.
[11] Vera N. Tesis Doctoral. Atlas climático de irradiación solar a partir de imágenes del satélite NOAA. Aplicación a la Península Ibérica. Universidad Politécnica de Cataluña. Barcelona España, Mayo; 2005.
[12] Yadav AK, Chandel SS. Solar energy potential assessment of western Himalayan Indian state of Himachal Pradesh using J48 algorithm of WEKA in ANN based prediction model. Renew Energy 2015;75:675–93.
[13] Sorapipatana C An. Assessment of solar energy potential in Kampuchea. Renew Sustain Energy Rev 2010;14:2174–8.
[14] Can Ertekin, Osman Yaldiz. Comparison of some existing models for estimating global solar radiation for Antalya (Turkey). Energy Conver Manag 2000;41:311–30, (Junio 1999).
[15] Khatib T, Mohamed A, Sopian K. A review of solar energy modeling techniques. Renew Sustain Energy Rev 2012;16(5):2864–9.
[16] El Ouderni AR, Maatallah T, El Alimi S, Nassrallah SB. Experimental assessment of the solar energy potential in the gulf of Tunis, Tunisia. Renew Sustain Energy Rev 2013;20:155–68.
[17] Comparative study of mathematical models in estimating solar irradiance for Australia.
[18] Sözen A, Arcakliogˇlu E. Effect of relative humidity on solar potential. Appl Energy 2005;82(4):345–67.
[19] Fadare DA. Modelling of solar energy potential in Nigeria using an artificial neural network model. Appl Energy 2009;86(9):1410–22.
[20] Sözen A, Arcaklioğlu E, Özalp M, Kanit EG. Use of artificial neural networks for mapping of solar potential in Turkey. Appl Energy 2004;77(3):273–86.
[21] Sözen A, Arcaklioğlu E. Solar potential in Turkey. Appl Energy 2005;80(1):35–45.
[22] Sözen A, Arcaklioğlu E, Özalp M, Kanit EG. Solar-energy potential in Turkey. Appl Energy 2005;80(4):367–81.
[23] Gutierrez-Corea FV, Manso-Callejo MA, Moreno-Regidor MP, Manrique-Sancho MT. Forecasting short-term solar irradiance based on artificial neural networks and data from neighboring meteorological stations. Sol Energy 2016;134:119–31.
[24] Pan T, Wu S, Dai E, Liu Y. Estimating the daily global solar radiation spatial distribution from diurnal temperature ranges over the Tibetan Plateau in China. Appl Energy 2013;107:384–93.
[25] Bristow KL, Campbell GS. On the relationship between incoming solar radiation and daily maximum and minimum temperature. Agric For Meteorol 1984;31(2):159–66.
[26] Grindley PC, Batty WJ, Probert SD. Mathematical model for predicting the magnitudes of total, diffuse, and direct-beam insolation. Appl Energy 1995;52(2):89–110.
[27] Liu Y, Shimada S, Yoshino J, Kobayashi T, Miwa Y, Furuta K. Ensemble forecasting of solar irradiance by applying a mesoscale meteorological model. Sol Energy 2016;136:597–605.
[28] Kurtz B, Kleissl J. Measuring diffuse, direct, and global irradiance using a sky imager. Sol Energy 2017;141:311–22.
[29] Lou S, Li DH, Lam JC, Chan WW. Prediction of diffuse solar irradiance using machine learning and multivariable regression. Appl Energy 2016;181:367–74.
[30] Chu Y, Coimbra CF. Short-term probabilistic forecasts for Direct Normal Irradiance. Renew Energy 2017;101:526–36.

[31] Bird R Hulstrom R. A simplified clear sky model for direct and diffuse insolation on horizontal surfaces. Solar Energy Research Institute, EEUU; 1981.
[32] Pinazo JM. Manual de Climatización, Tomo II. Universidad Politécnica de Valencia. ISBN 84-7721-341-0. España; 1995.
[33] Bosca JV. Tesis Doctoral: Contribución al estudio de la radiación solar y de la determinación de la turbiedad atmosférica. Aplicaciones a Valencia y Sevilla. Universidad Politécnica de Valencia. Valencia, España; 1995.
[34] Villicaña-Ortiz E, Gutiérrez-Trashorras AJ, Paredes-Sánchez JP, Xiberta-Bernat J. Solar energy potential in the coastal zone of the Gulf of Mexico. Renew Energy 2015;81:534–42.
[35] Hernández-Escobedo Q, Rodríguez-García E, Saldaña-Flores R, Fernández-García A, Manzano-Agugliaro F. Solar energy resource assessment in Mexican states along the Gulf of Mexico. Renew Sustain Energy Rev 2015;43:216–38.
[36] Rivas D, Saleme-Vila S, Ortega-Izaguirre R, Chalé-Lara F, Caballero-Briones F. A climatological estimate of incident solar energy in Tamaulipas, northeastern Mexico. Renew Energy 2013;60:293–301.
[37] Cancino SY, Gutiérrez-T A, Xiberta-B J. Current state of wind energy in Mexico, achievements and perspectives Review Article. Renew Sustain Energy Rev 2011;15(8), [3552-355].
[38] Estrada C Almanza R. Irradiaciones global, directa y difusa, en superficies horizontales e inclinadas, así como irradiación directa normal en la República Mexicana. Serie Investigación y Desarrollo. Instituto de Ingeniería de la UNAM. ISBN 970-32-0196-2. Mayo. México; 2005.
[39] Mapa de recurso solar. Sistema de Información Geográfica para las Energías renovables en México (SIGER). Instituto de Investigaciones Eléctricas (IIE). ⟨http://sag01.iie.org.mx/evaluarer/SIGER.html⟩ [Last Accessed April 2017].
[40] Estrada C, Cabanillas R, Hinojosa F, Pérez B, Ochoa M, Manrincic Irene, Regalado L. Ponencia Innovación para un futuro más brillante. Laboratorio Nacional de Sistemas de Concentración Solar y Química Solar UNISON-UNAM. Programa de transferencia de Tecnología TxTec. Abril. México; 2008.
[41] Agredano J. Prospectiva de las Tecnología Solar Fotovoltaica para la Generación de Electricidad. División de Energías Alternas. Instituto de Investigaciones Eléctricas (IIE). Anexo 7. México; 2005.
[42] Polo J, Gastón M, Vindel JM, Pagola I. Spatial variability and clustering of global solar irradiation in Vietnam from sunshine duration measurements. Renew Sustain Energy Rev 2015;42:1326–34.
[43] Nijegorodov N, Luhanga PVC. A new model to predict direct normal instantaneous solar radiation, based on laws of spectroscopy, kinetic theory and thermodynamics. Renew Energy 1998;13(4):523–30.
[44] Mohammadi K, Khorasanizadeh H. A review of solar radiation on vertically mounted solar surfaces and proper azimuth angles in six Iranian major cities. Renew Sustain Energy Rev 2015;47:504–18.
[45] Eltbaakh YA, Ruslan MH, Alghoul MA, Othman MY, Sopian K, Razykov TM. Solar attenuation by aerosols: an overview. Renew Sustain Energy Rev 2012;16(6):4264–76.
[46] Kudish AI, Evseev EG. The analysis of solar UVB radiation as a function of solar global radiation, ozone layer thickness and aerosol optical density. Renew Energy 2011;36(6):1854–60.
[47] Saffaripour MH, Mehrabian MA. Numerical methods applied to global solar radiation modeling – comparison with measured data. Int J Numer Methods Heat Fluid Flow 2009;19(6):777–89, [May 2008].
[48] Psiloglou BE, Santamouris M, Asimakopoulos DN. On broadband Rayleigh scattering in the atmosphere for solar radiation modelling. Renew Energy 1995;6(4):429–33.
[49] Psiloglou BE, Santamouris M, Asimakopoulos DN. Predicting the broadband transmittance of the uniformly mixed gases (CO 2, CO, N 2 O, CH 4 and O 2) in the atmosphere, for solar radiation models. Renew Energy 1995;6(1):63–70.
[50] Kataoka N, Yoshida S, Ueno S, Minemoto T. Evaluation of solar spectral irradiance distribution using an index from a limited range of the solar spectrum. Curr Appl Phys 2014;14(5):731–7.
[51] Nikitidou E, Kazantzidis A, Salamalikis V. The aerosol effect on direct normal irradiance in Europe under clear skies. Renew Energy 2014;68:475–84.
[52] Shaltout MM, Tadros MTY, El-Metwally M. Studying the extinction coefficient due to aerosol particles at different spectral bands in some regions at great Cairo. Renew Energy 2000;19(4):597–615.
[53] Moreno T, Aerosoles atmosféricos: problemas ambientales. Temas ambientales. ⟨www.aulados.net⟩ [Last Accessed April 2017].
[54] Tapakis R, Charalambides AG. Enhanced values of global irradiance due to the presence of clouds in Eastern Mediterranean. Renew Energy 2014;62:459–67.
[55] Hussain M, Khatun S, Rasul MG. Determination of atmospheric turbidity in Bangladesh. Renew Energy 2000;20(3):325–32.
[56] Eltbaakh YA, Ruslan MH, Alghoul MA, Othman MY, Sopian K. Issues concerning atmospheric turbidity indices. Renew Sustain Energy Rev 2012;16(8):6285–94.
[57] Carlos Toledano O. Tesis Doctoral: Climatología de los aerosoles mediante la caracterización de propiedades ópticas y masas de aire en la estación El Arenillo de la red Aeronet. Universidad de Valladolid. España; 2005.
[58] Kusienska B. Ponencia: La Concentración de Aerosoles en la Atmósfera inhibe la lluvia en la Ciudad de México. Departamento de Física de Nubes. UNAM-México. Boletín UNAM-DGCS-515. Agosto. México; 2009.
[59] Chaâbane M, Masmoudi M, Medhioub K. Determination of Linke turbidity factor from solar radiation measurement in northern Tunisia. Renew Energy 2004;29(13):2065–76.
[60] Raichijk C. Estimación del Índice de Turbidez de Linke para distintas Localidades de Argentina. GERSolar, Instituto de Ecologia y Desarrollo Sustentable (INEDES), Departamento de Ciencias Básicas. Argentina; 2009.
[61] Moon P. Proposed standard solar-radiation curves for engineering use. J Frankl Inst 1940:583–617.
[62] Fowle F. The transparency of aqueous vapor. Astrophys J 1915:394–411.
[63] Läuchli A. Zur absorption der ultravioletten Strahlung in Ozon. Z Phys Hadrons Nucl 1929:92–4.
[64] Reddy J. An an empirical method for the estimation of total solar radiation. Sol Energy 1971:289–90.
[65] IDEAM, Atlas de radiación solar de Colombia. República de Colombia: Centro de Documentación e Información Científica Técnica; 2005.
[66] ASHRAE, Handbook of fundamentals. New York; 1972.
[67] Threlkeld J. Direct solar radiation avaible on clear days. American Society of Heating, Refrigeration and Air Condition Engineers; 1958.
[68] Lacis A, Hansen J. A parametrization for the absorption in solar radiation in the Earth's Atmosphere. J Atmos Sci 1973:118–33.
[69] Manabe S, Strickler R. Thermal equilibrium in the atmosphere with a convective adjustment. J Atmos Sci 1964:361–85.
[70] Hottel H. A simple model for estimating the transmitance of direct solar radiation through clear atmospheres. Sol Energy 1976:129–34.
[71] Passamai V. Determinación de radiación solar horaria para dias claros mediante planila de cálculo. Facultad de Ciencias Exactas, Universidad Nacional de Salta, Argentina; 2000.
[72] Davies J. Calculation of the solar radiation incident on a horizontal surface. Canadian Atmospheric Enviroment Service. Proceedings of the First Canadian Solar Radiation Data Workshop; 1979.
[73] Hoyt D. A model for calculation of solar global insolation. Sol Energy 1978:27–35.
[74] Yamamoto G. Direct absorption of solar radiation by atmospheric water vapor, carbon dioxide and molecular oxigen. J Atmos Sci 1962:182–8.
[75] Burch D. Total absortance in carbon dioxide in the infrared. Appl Opt 1962:759–65.
[76] Angstrom A. Techniques of determining the turbidity of the atmosphere. The Eppley Foundation for Research. Tellus XIII; 1961.
[77] Angstrom A. The parameters of atmospheric turbidity. The Eppley Foundation for Research. Tellus XVI; 1964.
[78] Atwater M, Ball J. A surface solar radiation model for cloudy atmosphere. Mon Weather Rev 1980:879–88.
[79] Mcdonald J. Direct absorption of solar radiation by atmospheric water vapor. J Meteorol 1960:319–28.
[80] Watt O. On the nature and distribution of solar radiation. Departamento de Energía de EEUU; 1975.
[81] Valley S. Handbook of geophysics and space enviroments. Air Force Cambridge Research Lans Hanscom; 1965.
[82] Wong LT, Chow WK. Solar radiation model. Appl Energy 2001;69(3):191–224.
[83] Carlos Toledano O. Tesis Doctoral: Climatología de los aerosoles mediante la caracterización de propiedades ópticas y masas de aire en la estación El Arenillo de la red Aeronet. Universidad de Valladolid. España; 2005.
[84] Mächler M. Tesis de maestría: Parametrization of solar irradiation under clear skies. Departamento de Ingeniería Mecánica, Universidad de Columbia. Vancouver, Canadá; 1983.
[85] Mächler M. Tesis de maestría: Parametrization of solar irradiation under clear skies. Departamento de Ingeniería Mecánica, Universidad de Columbia. Vancouver, Canadá; 1983.
[86] SMN, Sistema Meteorológico Nacional, Red de observatorios meteorológicos (1981–2010). Normales climatológicas; 2010–2011. ⟨http://smn.cna.gob.mx/esmas⟩. Acceso a la información en.
[87] INEGI. Instituto Nacional de Estadística y Geografía. Mapoteca Digital Versión 2.0. ⟨http://www.inegi.org.mx⟩.
[88] Jáuregui E. Algunas altereaciones de largo periodo del clima de la Ciudad de México debidas a la urbanización. Departamento de Meteorología General, Centro de Ciencias de la Atmósfera, UNAM. México; 1995.
[89] Gueymard C. Critical analisys and performance asserrment of clear sky solar irradiance models using theorical ans measured data. Sol Energy 1993:121–38.
[90] Wright J. Correlaciones de la fracción difusa. Tópicos Meteor Oceano 2000:15–8.
[91] Collares M, Rabl . The average distribution of solar radiation-correlation between difusse and hemispherical and daily and hourly insolation values. Sol Energy 1979:155–64.
[92] Orgill J, Hollands G. Correlation equation for hourly difusse radiation on horizontal surface. Sol Energy 1977:357–9.
[93] Erbs G, Klein S, Duffie J, et al. Estimation of the difusse radiation fraction fou hourly, daily and monthly average global radiation. Sol Energy 1982:293–304.
[94] Spencer J. A comparison of methods for estimating hourly difusse solar radiation from global solar radiation. Sol Energy 1982:19–32.
[95] Garcia G, Velarde J. Energías Renovables y Medio Ambiente. Centro de Estudios de Ordenación del Territorio y Medio. Ambiente. España; 1982.
[96] Tung CP, Yang YCE, Lee TY, Li MH. Modification of a stream temperature model with Beer's law and application to GaoShan Creek in Taiwan. Ecol Model 2007;200(1):217–24.
[97] Forero N, Caicedo L, Gordillo G. Correlation of global solar radiation values estimated and measured on an inclined surface for clear days in Bogotá. Renew Energy 2007:2590–602.
[98] Mapa Hipsográfico y de México Batimétrico. Instituto de Geografía, Universidad Autónoma de México. INEGI. México Junio.